Developmental Cell, Vol. 9, 415–422, September, 2005, Copyright ©2005 by Elsevier Inc. DOI 10.1016/j.devcel.2005.08.002

Regulatory Mutations of *mir-48*, a *C. elegans let-7* Family MicroRNA, Cause Developmental Timing Defects

Short Article

Ming Li,[1] Matthew W. Jones-Rhoades,[2] Nelson C. Lau,[2,3] David P. Bartel,[2] and Ann E. Rougvie[1,*]
[1]Department of Genetics
Cell Biology and Development
University of Minnesota
6-160 Jackson Hall
321 Church Street, SE
Minneapolis, Minnesota 55455
[2]Whitehead Institute for Biomedical Research and
Department of Biology
Massachusetts Institute of Technology
9 Cambridge Center
Cambridge, Massachusetts 02142

Summary

The *C. elegans* heterochronic genes program stage-specific temporal identities in multiple tissues during larval development. These genes include the first two miRNA-encoding genes discovered, *lin-4* and *let-7*. We show that *lin-58* alleles, identified as *lin-4* suppressors, define another miRNA that controls developmental time. These alleles are unique in that they contain point mutations in a gene regulatory element of *mir-48*, a *let-7* family member. *mir-48* is expressed prematurely in *lin-58* mutants, whereas expression of *mir-241*, another *let-7* family member residing immediately upstream of *mir-48*, appears to be unaffected. A *mir-48* transgene bearing a *lin-58* point mutation causes strong precocious phenotypes in the hypodermis and vulva when expressed from multicopy arrays. *mir-48::gfp* fusions reveal expression in these tissues, and inclusion of a *lin-58* mutation causes precocious and enhanced *gfp* expression. These results suggest that *lin-58* alleles disrupt a repressor binding site that restricts the time of miR-48 action in wild-type animals.

Introduction

The heterochronic genes of *C. elegans* are global temporal regulators that specify the proper timing and sequence of several events during larval development (reviewed in Rougvie, 2001). These events include behaviors of hypodermal seam cells, which divide in stage-specific patterns until the final (L4) molt, when they terminally differentiate. Mutations in heterochronic genes cause seam cells to adopt temporal identities normally restricted to a different life stage, resulting in omission or reiteration of stage-specific division patterns. Most of these genes can be broadly classified as components of an "early timer" that directs successive cell fates from the L1 to the L3 stage or a "late timer" that then guides development through to the adult stage.

The two founding members of the miRNA gene family, *lin-4* and *let-7*, play key roles in the heterochronic gene pathway by initiating the early and late timers, respectively. *lin-4* is activated in the mid-L1 stage and downregulates LIN-28 and LIN-14 accumulation through complementary sites in the 3′ UTRs of their mRNAs (Feinbaum and Ambros, 1999; Lee et al., 1993; Moss et al., 1997; Wightman et al., 1993). The progressive decay in LIN-14 and LIN-28 levels specifies hypodermal seam cell fates during early development. LIN-14 specifies L1 fates and then, together with LIN-28, prevents L3-stage fates from occurring precociously in the L2 stage and thereby allows a proliferative seam cell division to occur. *let-7* miRNA accumulates during the L3 stage and advances seam cell fates through the final larval stage to the adult by downregulation of targets including *lin-41* (Reinhart et al., 2000; Slack et al., 2000), which is required to prevent adult fates during the fourth larval stage.

Identification and analysis of worm miRNAs has revealed three temporally regulated *let-7* homologs (*mir-48*, *mir-84*, and *mir-241*), raising the possibility of partial functional redundancy among this gene family (Lau et al., 2001; Lim et al., 2003). The 5′ eight nucleotides of the mature miRNAs are identical among the four *let-7* family members, and this region is generally the most conserved portion of metazoan miRNA homologs, suggesting that it is key for target recognition (for a review, see Bartel, 2004). Indeed, perfect Watson-Crick pairing to the 5′ "seed" region of the miRNA (nucleotides 2–7 or 2–8) is important and sufficient for accurate prediction of miRNA targets and for regulation of reporter constructs (Brennecke et al., 2005; Doench and Sharp, 2004; Krek et al., 2005; Lewis et al., 2003, 2005; Lim et al., 2005). Therefore, the identical seed sequences of the four *let-7* family members indicate that they could act through similar or overlapping sets of binding sites and regulate common targets if temporally and spatially coexpressed. This redundancy could explain why the heterochronic gene *hbl-1*, which appears to be a *let-7* target (its 3′ UTR contains multiple potential *let-7* binding sites, and it exhibits partial redundancy with *lin-41* downstream of *let-7*), remains properly regulated in the hypodermis of *let-7* mutants (Abrahante et al., 2003; Lin et al., 2003). *let-7* family member binding sites have also been identified in the 3′ UTRs of other heterochronic genes (Reinhart et al., 2000).

We previously isolated *lin-58* alleles as suppressors of the *lin-4* retarded hypodermal phenotype. On their own, *lin-58* mutants are similar to wild-type in overall appearance, but they have a weak precocious hypodermal phenotype (Abrahante et al., 1998). We demonstrate here that this phenotype is due to precocious expression of miR-48. These results define a heterochronic role for *mir-48*, and they identify a regulatory element through which the timing of miR-48 accumulation is controlled.

*Correspondence: rougvie@biosci.cbs.umn.edu
[3]Present address: Department of Molecular Biology, Massachusetts General Hospital, 55 Fruit Street, Boston, Massachusetts 02114.

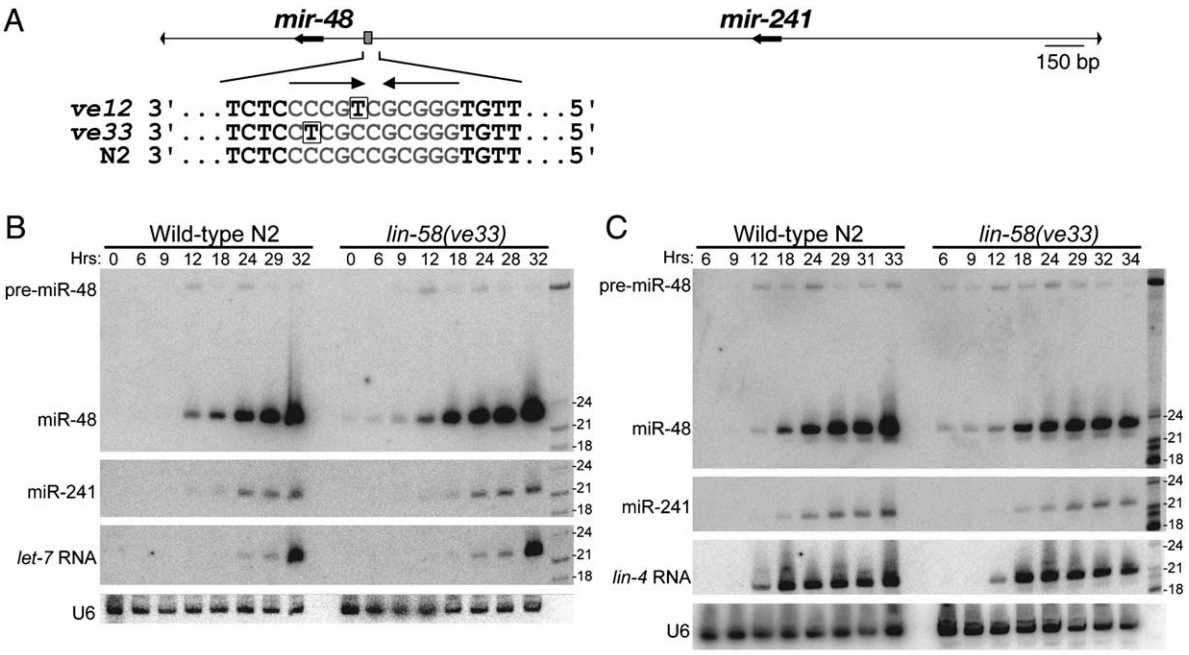

Figure 1. *lin-58* Alleles Contain *mir-48* Gene Regulatory Lesions that Cause Precocious Expression

(A) The *mir-48* and *mir-241* loci on chromosome V are diagrammed with the *lin-58(ve12)* and *lin-58(ve33)* point mutations shown below.
(B and C) Northern blot analyses of total RNA from synchronous populations of wild-type (left) or *lin-58(ve33)* mutant animals (right) at the indicated number of hours after placement of L1 hatchlings on food. For miR-241, *let-7*, and *lin-4* miRNAs, only the bands representing mature miRNAs are shown. The blots were probed sequentially for the indicated RNAs with U6 snRNA as a loading control. The L1 molt corresponds to 18 hr, and the L2 molt corresponds to 29 hr, except in the *lin-58* portion of (B), where it was 28 hr.

Results

lin-58 Alleles Contain miRNA Gene Regulatory Mutations

lin-58 maps to an approximately 1.2 cM interval of linkage group V between *him-5* and *unc-76* (Abrahante et al., 1998). Two miRNAs of the *let-7* gene family, *mir-48* and *mir-241*, reside in tandem within this region (Lau et al., 2001; Lim et al., 2003), raising the possibility that these miRNA genes might harbor the *lin-58* mutations. Sequence analysis revealed that the mature *mir-48* and *mir-241* miRNAs, and their pre-miRNAs, were wild-type in *lin-58* mutant animals. However, these *lin-58* alleles could contain gene regulatory mutations, a tantalizing possibility given the semidominant nature of the stronger allele, *ve33* (Abrahante et al., 1998). Indeed, sequence analysis of flanking regions, including the 1.7 kb between the two miRNA coding regions, identified a distinct point mutation in each allele. These two independent point mutations were 3 bp apart and were located within a GC-rich inverted repeat approximately 210 bp upstream of the miR-48 coding sequence and 1540 bp downstream of the miR-241 coding sequence (Figure 1A). These mutations were not simply strain polymorphisms; they were not present in the parental strain used for the mutagenesis, nor were they present in three independent mutants isolated from the same screen (data not shown). Rather, they are likely to be miRNA gene regulatory mutations, the first, to our knowledge, such point mutations to be identified from a genetic screen.

miR-48 Accumulates Precociously in *lin-58(ve33)* Mutants

The precocious phenotype of *lin-58* mutants (Abrahante et al., 1998) suggests that the *ve12* and *ve33* lesions disrupt a negative regulatory element, resulting in premature expression of *mir-48* and/or *mir-241* and the consequent early downregulation of their target genes. To test this hypothesis, we performed developmental Northern blots of total RNA isolated from synchronously staged populations of mutants bearing the stronger allele, *ve33*, versus wild-type. The 23 nt mature miR-48 and its ~60 nt precursor were readily detected at 18 hr postembryogenesis (and weakly at 12 hr) in two independently staged populations of wild-type animals (Figures 1B and 1C). In contrast, these RNAs were detected at 6 hr in RNA samples isolated from *ve33* mutants, a time at which miR-48 was undetectable in wild-type. miR-48 was also detectable in *ve33* L1 animals synchronized by starvation prior to exposure to food (i.e., at time "0"; Figure 1B). When quantitated relative to U6 snRNA loading controls, miR-48 expression was at least 2-fold to 6-fold higher in *ve33* animals relative to wild-type at 0, 6, and 9 hr (see Experimental Procedures). The *mir-48* pre-miRNA was detected at 12 hr in *ve33* mutants in a ratio to mature miR-48 that was similar to that of wild-type at the same stage. This result suggests that pre-miR-48 processing was not compromised by the *ve33* lesion.

Reprobing of the Northern blots for miR-241 showed little, if any, difference in miR-241 accumulation relative to wild-type (Figures 1B and 1C), suggesting that *mir-*

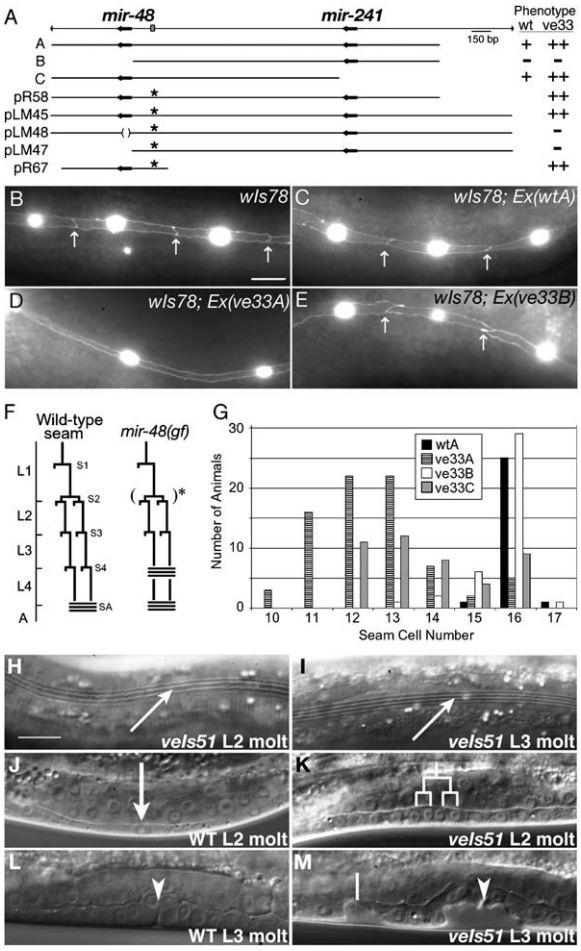

Figure 2. *mir-48* Misexpression Phenotypes

(A) PCR-generated fragments A, B, and C and genomic clones are diagrammed relative to the *mir-48/mir-241* loci. The columns to the right indicate whether the construct caused a precocious hypodermal phenotype in transgenic animals. +, ++, strength of phenotype; –, little or no phenotype. wt and ve33 indicate whether the test fragment was amplified from wild-type or *lin-58(ve33)* mutant animals, respectively. The asterisks indicate where the *ve33* lesion is present. The parentheses indicate that the 23 nt corresponding to mature miR-48 were deleted.

(B–E) AJM-1::GFP and SCM::GFP expressed from *wIs78* label adherens junctions and seam cell nuclei, respectively, in L3 molt animals bearing extrachromosomal arrays of the indicated PCR fragments. Arrows indicate contacts between unfused seam cells in (B), (C), and (E). The scale bar is 10 μm. (C) *wIs78; veEx361*. (D) Precociously fused seam cells in a *wIs78; veEx230* animal. (E) *wIs78; veEx236*.

(F) V1–V4 seam cell lineage pattern in wild-type and *mir-48* overexpression strains. The asterisk indicates that the proliferative S2 division is sometimes skipped in the *mir-48(gf)* strains, resulting in fewer seam cells with increased spacing as in (D).

(G) Graph showing distribution of seam cell number in adults (Table S1). At hatching, each strain appeared to be wild-type, with ten seam cells per side. In wild-type, 6 seam cell lineages undergo the proliferative S2 division at the L1 molt, increasing the seam cell number to 16.

(H and I) Precocious adult alae (arrows) in *vels51* animals, which bear a pR58-containing array, at the (H) L2 and (I) L3 molts. The scale bar is 10 μm.

(J–M) Precocious vulva development in *vels51* animals. (J and K) VPCs of L2 molt animals. (J) The arrow indicates the undivided P6.p cell in wild-type. (K) Two rounds of P6.p division occurred in a *vels51* animal. P5.p and P7.p had also divided in this animal, but their lineages were not followed. Vulva morphogenesis in L3 molt-stage wild-type (L) and *vels51* (M) animals. Vulva formation is advanced in *vels51*, and invaginations are often abnormal. Pseudovulval invaginations are also sometimes seen (line).

48 misexpression was largely responsible for the observed *lin-58* precocious phenotype. Although previous analyses have reported that *let-7* miRNA accumulation begins at the L3 stage (Lau et al., 2001; Reinhart et al., 2000), the sensitivity of this Northern, coupled to the sampling of multiple time points per stage, revealed low levels of *let-7* miRNA during the L2 stage (24 hr), with significant upregulation during the L3 stage in both wild-type and *lin-58* mutants (Figure 1B).

As an additional control, the blot in Figure 1C was probed for the *lin-4* miRNA, which acts upstream of *lin-58* in the heterochronic gene pathway (Abrahante et al., 1998) and should thus be unaffected by *lin-58* mutation. Its temporal expression profile was not accelerated by the *ve33* lesion. Thus, the observed temporal shift in miR-48 accumulation in *ve33* mutants relative to wild-type was not due to a lack of developmental synchrony in the nematode populations. Rather, *mir-48* expression was precocious in *lin-58* mutants.

Overexpression of *mir-48* in Transgenic Animals Causes Precocious Seam Cell Phenotypes

To further test the effects of the *lin-58(ve33)* lesion on expression from the *mir-48/mir-241* locus, we assayed the phenotypes of transgenic animals bearing PCR-amplified genomic fragments or plasmid subclones (Figure 2A) from either wild-type or *lin-58(ve33)* mutant DNA. Three stage-specific events were monitored for heterochronic defects in the hypodermis: seam cell fusion and adult cuticular alae synthesis, which normally occur at the end of the L4 stage during the transition to the adult, and an earlier event, the execution of the proliferative "S2" seam cell division, which follows the L1 molt in wild-type animals (see Figure 2F; Ambros and Horvitz, 1984). When assayed by seam cell fusion, three of four transgenic lines bearing the amplified wtA fragment (or its plasmid clone pR56), which encompasses both miRNAs, showed no precocious seam cell fusion at the L3 molt ($n \geq 20$ for each line; Figure 2C; Table S1; see the Supplemental Data available with this article online). A low level of precocious fusion was observed in the fourth line (3%), as might be expected due to overexpression of the wild-type locus from multicopy arrays. In contrast, the seam cell fusion phenotype was dramatically enhanced, to nearly 100% penetrance, by inclusion of the *ve33* lesion in the construct (ve33A; Figure 2D; Table S1). This finding is consistent with this mutation causing precocious miRNA expression. Precocious alae formation was also observed in animals containing wtA or ve33A arrays (Table 1; Figures 2H and 2I). Animals transgenic for ve33A had a stronger phenotype than that caused by the *ve12* and *ve33* alleles; although still often not full-length, the precocious alae were more robust and distinct, consistent with enhanced expression from multicopy arrays. Finally, the proliferative S2 division executed by a subset of seam

Table 1. *mir-48* Arrays Cause Precocious Adult Cuticle and Vulval Phenotypes

Genotype	Construct[a]	Percentage of Animals with Adult Alae Formation			VPC Division at L2 Molt (%)[c]
		L2 Molt[b]	L3 Molt[b]	L4 Molt[b]	
Wild-type	—	0	0	100	0
veEx254	wtA	nd	33 (100)	nd	nd
veEx258	wtA	nd	38 (78)	nd	nd
veEx256	wtB	nd	0	nd	nd
veEx249	wtB	nd	0	nd	nd
veEx257	wtC	nd	32 (86)	nd	nd
veEx242	wtC	nd	21 (100)[d]	nd	nd
veEx233	ve33A	nd	31 (83)	nd	nd
veEx243	ve33A	nd	57 (62)	nd	nd
veEx244	ve33B	nd	0	nd	nd
veEx332	pLM45	nd	63 (50)	nd	nd
veEx335	pLM45	nd	19 (100)	nd	nd
veEx326	pLM48	nd	0	nd	nd
veEx336	pLM47	nd	0	nd	nd
veEx337	pLM47	nd	0	nd	nd
veEx327	pR67	nd	38 (90)	nd	nd
vels49	ve33A	4 (100)	100 (27)	nd	79
vels40	ve33C	0[d]	100 (17)	nd	43
vels48	ve33C	28 (83)	100 (45)	nd	81
vels51	pR58	39 (83)	100 (26)	nd	87
let-7[e]	—	0	0	10 (10)	0
vels51 let-7[e]	pR58	0	76 (56)	100 (35)	65

Note: n ≥ 20 animals unless otherwise noted. nd, not determined.
[a] PCR fragments (1 ng/μl) and plasmid clones (5 ng/μl) were coinjected with *sur-5::gfp* (50 ng/μl) (Yochem et al., 1998).
[b] For animals with alae, the percentage that had incomplete alae containing gaps is given in parentheses.
[c] Percentage of animals with at least one VPC division at the L2 molt.
[d] n = 14.
[e] *unc-3(e151)* is tightly linked to *let-7* and is present in the background (see Experimental Procedures).

cells following the L1 molt was often skipped in animals bearing ve33A arrays relative to wtA, resulting in a lower seam cell number in adults (Figure 2G; Table S1). This result suggests that targets of miR-48 and/or miR-241 act in the early timer to specify this event.

Analysis of deletion constructs and shorter PCR fragments indicated that *mir-48* misexpression was the key factor in the precocious hypodermal phenotypes produced in these transgenic animals. Removal of *mir-241* did not appreciably alter the precocious alae phenotype and had little effect on seam cell number (PCR product C, pR67; Table 1; Table S1; Figure 2G). In contrast, deletion of *mir-48*, including a 23 bp deletion of the mature miR-48 coding sequence, resulted in little or no phenotype when assayed in transgenic animals (PCR product B, pLM47, and pLM48; Figures 2E and 2G; Table 1; Table S1).

Integration of extrachromosomal arrays bearing ve33A or ve33C into the genome to obtain strains that stably transmit the transgene array (*vels40*, *vels48*, *vels49*, and *vels51* in Table 1) resulted in enhanced penetrance of the precocious alae phenotype, with 100% of animals synthesizing adult cuticle at the L3 molt. Moreover, three of these strains synthesized adult cuticle at the L2 molt, two stages earlier than in wild-type (Table 1; Figure 2H). One of these strains, *vels48*, lacked *mir-241*, indicating that *mir-48* misexpression was also sufficient to confer this precocious phenotype.

Multicopy Arrays Containing *mir-48* Cause Precocious Division of Vulva Precursor Cells

Extrachromosomal arrays containing ve33A or ve33C also produced a low penetrance protruding vulva phenotype. When integrated, a severe and fully penetrant egg-laying defect was observed: the animals did not lay eggs (n > 100). Examination of the vulval cell lineage in these animals revealed a cell division timing defect. In wild-type animals, three of six vulval precursor cells (VPCs) are induced to divide in the mid-to-late L3 stage, generating 22 cells that form the vulva (Sulston and Horvitz, 1977). VPC divisions often occurred during the L2 stage in ve33A and ve33C transgenic animals, and a second pseudovulva was sometimes seen (Table 1; Figures 2J–2M), suggesting that additional VPCs may be induced to a vulval cell fate in these animals. Precocious VPC divisions were not observed in L2 molt animals bearing ve33B (n = 10), indicating that miR-48 was required for this phenotype.

mir-48::gfp Expression in the Hypodermal Seam and Vulva Is Enhanced and Temporally Shifted by the *ve33* Lesion

mir-48::gfp fusions were used to test whether inclusion of the *ve33* lesion alters the resulting temporal expression pattern (Figure 3). *gfp* expression was detected in the lateral hypodermal seam and the vulva beginning during the L4 stage, when driven by a wild-type fragment extending 1.0 kb upstream from the miR-48 coding sequence (*mir-48::gfp*). A single head neuron, RID, also consistently expressed *gfp*, but did so in a non-temporally regulated fashion and served as an internal control (Figures 3J and 3O). *mir-48(Δ)::gfp* gave a similar pattern (Figure 3A; data not shown).

Introduction of the *ve33* lesion into *mir-48::gfp* resulted in precocious and enhanced *gfp* expression in the seam and vulva (*mir-48(ve33)::gfp*; Figure 3). *mir-*

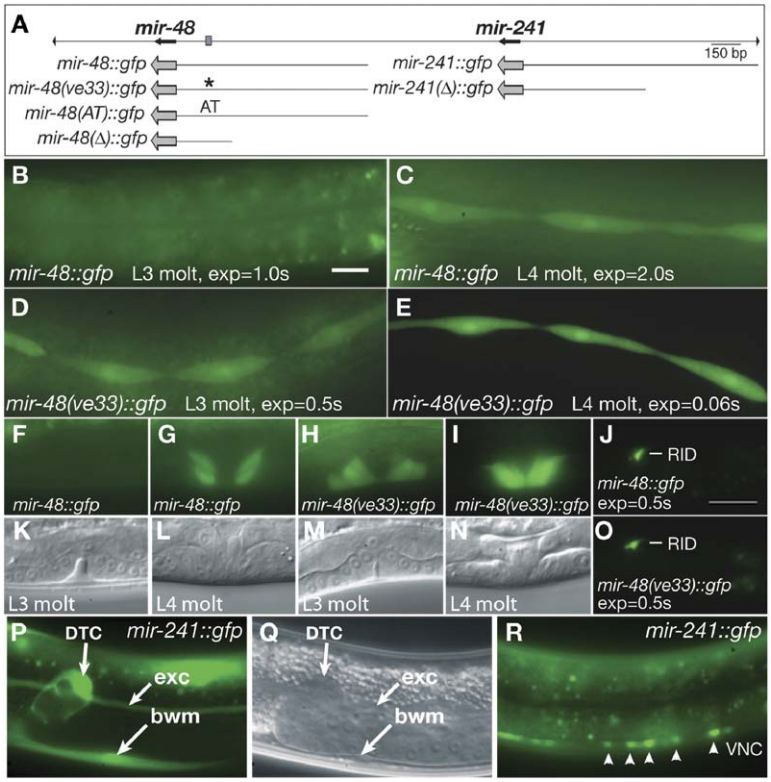

Figure 3. Expression of *mir-48::gfp* and *mir-241::gfp* Fusions

(A) *mir-48* and *mir-241 gfp* fusions are diagrammed. Gray arrows indicate the GFP coding sequence. "AT" indicates that the inverted repeat was replaced with an AT-rich sequence. The asterisk indicates the *ve33* lesion.

(B–R) Representative *gfp* expression patterns. Where especially relevant, exposure times are indicated in the panels (exp). (B) *mir-48::gfp* expression is not detected in L3 molt animals, but is readily detected at the (C) L4 molt. (D and E) The *ve33* lesion in *mir-48(ve33)::gfp* results in enhanced *gfp* expression that is detectable one stage earlier. (F–I) *gfp* is expression in descendents of P5.p and P7.p in the vulva. Corresponding Nomarski DIC images are shown in (K)–(N). *mir-48::gfp* is not detected at the L3 molt ([F]; exp = 2.0 s), but is present at the L4 molt ([G]; exp = 1.0 s). *mir-48(ve33)::gfp* is detected in the L3 stage ([H]; exp = 0.5 s) and more strongly at the L4 molt ([I]; exp = 0.06 s). (J and O) L2-stage RID expression in *mir-48::gfp* and *mir-48(ve33)::gfp*, respectively. (P–R) *mir-241::gfp* is expressed in a variety of cell types as indicated for the (P) L3 and (R) L2 stages. (Q) is the Nomarski DIC image corresponding to (P). The bar in (B) is 10 μm and applies to all panels except (J) and (O); the bar in (J) is 20 μm. Stage-nonspecific expression was observed in unidentified neurons in the head, tail, and ventral nerve cord for both *mir-48* and *mir-241* constructs.

48(ve33)::gfp expression in these tissues was stronger than that of *mir-48::gfp* and was consistently detected one stage earlier, in L3 larvae, with occasional seam expression detected in L2-stage animals. This change in timing and amplitude of *gfp* expression was not likely to reflect a difference in copy number between the strains because the results were consistent across multiple, independent transgenic lines (five for wild-type and four for *ve33*; data not shown). Although expression levels varied somewhat between lines generated with the same construct, expression of the wild-type construct was never detected in the L3 hypodermis, even when lines matched for RID expression levels were compared. Enhanced and precocious expression was also observed when the 11 bp GC-rich inverted repeat was replaced by an AT-rich sequence (GGG CGCCGCCC → ATTTATTATAA). Thus, the observed phenotypes of *lin-58(ve33)* mutants, and *mir-48* overexpression in transgenic worms, were due to temporal rather than spatial misexpression.

Multiple, independent assays, including phenotypic and Northern blot analysis of *lin-58* mutants, multicopy *mir-48* expression, and *mir-48::gfp* fusion analyses, all indicated that the GC element temporally controls miR-48 accumulation; its mutation shifted expression to earlier developmental times. However, there was a discrepancy in the time of first appearance of the GFP signal versus *mir-48* expression detected by Northern blot analysis. The reason for this difference is unclear, but it may be that additional transcriptional control elements were missing from the constructs. The *gfp* fusions assayed did contain sufficient 5′ sequences to produce a *mir-48* misexpression phenotype when present in a genomic DNA construct (pR67; Figure 2A; Table 1). Therefore, control elements missing from the *gfp* fusions might reside within or downstream of the sequences encoding the miR-48 stem loop. Regardless, the presence of the *ve33* lesion had a consistent effect in four different assays: it caused precocious *mir-48* expression, suggesting that the GC element defines a repressor binding site.

mir-241::gfp Expression Is Largely Distinct from *mir-48::gfp*

A *mir-241::gfp* fusion containing 1.3 kb 5′ to the miR-241 coding sequence resulted in a temporally regulated, but largely spatially distinct, expression pattern from that of *mir-48* (Figures 3P–3R). Notably, hypodermal expression was not consistently observed. Body-wall muscle expression was first detected in L2-stage animals and continued to the adult stage. In the L3 stage, expression was detected in the excretory canal and the distal tip cells, and strong vulval expression was observed during the L4 stage. No expression was observed in *mir-241(Δ)::gfp*, which retains 0.73 kb of 5′ sequence, indicating that regulatory sequences are present further upstream than for *mir-48*.

mir-48 Overexpression Partially Suppresses *let-7(lf)*

let-7 loss-of-function causes a retarded hypodermal phenotype in which animals synthesize larval-type, rather than adult-type, cuticle during the fourth molt;

animals then die by bursting at the vulva prior to producing progeny (Reinhart et al., 2000). Because the hypodermal phenotype is essentially opposite from that of *mir-48(gf)*, we examined the phenotype of *vels51 let-7(mn112)* animals. The retarded hypodermal phenotype associated with loss of *let-7* function was suppressed at the L4 molt (Table 1), and lethality decreased from 100% for *let-7* alone to 20% for *vels51 let-7* animals (n = 20). One possible interpretation of these results is that *mir-48* and *let-7* miRNAs share at least some targets during larval development and that overexpression of *mir-48* can compensate for loss of *let-7* activity. At earlier stages, precocious phenotypes caused by *mir-48(gf)* were still observed; however, the absence of *let-7* from the *vels51* background lessened the effect of *mir-48* overexpression, indicating that *let-7* functions in the L2-stage seam (Table 1). This decrease in phenotype severity also suggests common targets for these miRNAs.

Discussion

We demonstrate that *mir-48*, a member of the *let-7* miRNA family, acts in the heterochronic gene pathway to time cell fate decisions in the hypodermis and vulva. The number of miRNA genes acting in this timing pathway now stands at five: *lin-4* plus all four *let-7* family members (Abbott et al., 2005, in this issue of *Developmental Cell*; Johnson et al., 2005; Lee et al., 1993; Reinhart et al., 2000). In addition, the existence of miR-237, which is temporally expressed during larval development and has the same seed as the *lin-4* miRNA, suggests that at least six miRNAs may play a role in this pathway (Ambros et al., 2003; Lim et al., 2003).

Why do so many miRNAs act within the heterochronic gene pathway? Combinatorial action of animal miRNAs, analogous to that observed for transcription factors, has been proposed as a mechanism for increasing the complexity of gene expression patterns and the diversity of cell type (Bartel and Chen, 2004; Hobert, 2004). Similarly, in the heterochronic gene pathway, combinatorial action of miRNAs in the temporal dimension could act to specify changes in identity of a given cell over time. The potential exists for a given heterochronic gene to be regulated by multiple miRNAs acting through distinct, common, or overlapping sets of target sites, ultimately facilitating a precise pattern of temporal decay. Thus, the combined action of multiple miRNAs could fine tune expression of key proteins that temporally pattern development.

Similar to *lin-4* and *let-7* (Lee et al., 1993; Reinhart et al., 2000), our identification of *mir-48* as a developmental timing gene came from a forward genetics approach; however, in this case, there is a unique twist. Two *lin-4* suppressors contained distinct point mutations in a regulatory element upstream of mir-48 coding sequence, resulting in a gain-of-function, rather than loss-of-function, phenotype. The small size of miRNAs renders them poor targets for chemical mutagenesis. Transcription factor binding sites are generally smaller yet and often contain nucleotide positions at which degeneracy is allowed, making them even less likely to be targets for mutation. Nevertheless, our screen identified two such alleles that appear to have revealed a miRNA regulatory element. In fact, the gain-of-function nature of these alleles was instrumental in the identification of *mir-48* through a forward genetics approach because *mir-48* loss-of-function was also likely to be missed in screens due to genetic redundancy. *mir-48(null)* mutants have no seam cell phenotype, and there is little, if any, visible phenotype at standard screening temperatures, although an additional molt is seen at low temperature (Abbott et al., 2005).

Other types of regulatory mutations have also aided in miRNA gene discovery. Two of three *let-7* deletion alleles remove sequences 5′ to the pre-miRNA and cause loss-of-function phenotypes by disrupting processing of the primary transcript (Bracht et al., 2004; Reinhart et al., 2000). In plants, miR-319 was identified through gain-of-function alleles, in which promoter insertions of the 35S viral enhancer caused overexpression of the miRNA (Palatnik et al., 2003). In flies, identification of the miRNA *bantam* used a combination of loss-of-function and gain-of-function alleles, in which the locus was deleted or overexpressed, respectively, due to specially engineered P element insertions (Brennecke et al., 2003).

The time of accumulation of miR-48 in wild-type animals suggests that it acts to downregulate early timer components. Although our studies examine *mir-48* gain-of-function situations, the observed phenotypes are likely to reflect interactions with true target mRNAs, which are simply downregulated prematurely. Two main observations support this conclusion. First, the *ve33* lesion caused ectopic production of miR-48 in a temporal, but not spatial, dimension. Second, analysis of *mir-48* overexpression strains revealed that seam cells often skip the proliferative S2 division, a phenotype opposite to that implied from loss-of-function studies. Although *mir-48(lf)* does not reveal a seam cell phenotype, a double mutant combination with *mir-241(lf)* reveals reiteration of the S2 division, implying that these genes function redundantly to restrict this event to the early L2 stage (Abbott et al., 2005). Importantly, the opposite phenotypes observed for *mir-48(lf)* and *mir-48(gf)* suggest that the same or overlapping sets of target genes are affected in each situation. Although the constructs analyzed in our studies do not identify a major role for *mir-241*, constructs overexpressing *mir-241*, but not *mir-48*, occasionally had fewer seam cells than wild-type (Figure 2G).

Omission of the S2 division observed in *mir-48* overexpression studies suggests that two early timer genes may be direct targets of miR-48. *lin-28* (Ambros and Horvitz, 1984) or *hbl-1* (Abrahante et al., 2003) loss of function also results in omission of S2 divisions. In addition, the 3′ UTRs of their mRNAs have predicted *let-7* family member binding sites, and expression studies are consistent with *mir-48*-mediated downregulation (Abrahante et al., 2003; Lin et al., 2003; Reinhart et al., 2000; Seggerson et al., 2002). However, our previous studies indicate that *lin-28* cannot be the sole target of miR-48, because the *ve33* lesion can enhance the precocious phenotype of a *lin-28* null allele (Abrahante et al., 1998). *lin-28* is also not likely to be the major target of miR-48, because we did not observe suppression of *mir-48* overexpression phenotypes in a

lin-46 mutant background (data not shown), which eliminates the requirement for *lin-28* in the hypodermis and vulva (Pepper et al., 2004). Thus, although *lin-28* could play a minor role as a miR-48 target, we favor a model in which *hbl-1* is a key target in the hypodermis.

mir-48 misexpression also caused developmental timing defects, which include early P6.p division, in the vulva. However, we have not observed *mir-48::gfp* in the P6.p lineage, and, thus, *mir-48* may be expressed here at low levels, or it may time this division cell nonautonomously. Although we have not observed precocious VPC divisions in *lin-58(ve33)* or *lin-58(ve12)* mutant animals, these alleles do cause a synthetic vulval phenotype in double mutant combinations with the heterochronic gene *lin-42* (Abrahante et al., 1998). Inclusion of the *ve33* lesion in *mir-48(ve33)::gfp* led to enhanced and precocious vulval *gfp* expression, as in the hypodermis, indicating that the regulatory element is functioning in both tissues. Loss of function of the heterochronic genes *hbl-1*, *lin-28*, or *lin-14* result in precocious VPC divisions (Abrahante et al., 2003; Ambros and Horvitz, 1984) and could be targets of miR-48 in the vulva, as could *let-60*, a vulval target of the *let-7* family member miR-84 (Johnson et al., 2005).

The *lin-58* mutations described here appear to reveal a negative regulatory element that prevents *mir-48* accumulation until the proper time during the mid-to-late L1 stage. Intriguingly, the 11 bp inverted repeat disrupted by *lin-58* mutations (Figure 1) spans a 7–8 bp match to a computationally identified consensus motif (5′-CTCCGCCC-3′; underlined residues are mutated in *lin-58* alleles) found 5′ to most worm miRNA genes that are independently expressed (Ohler et al., 2004). A perfect match to this sequence also resides another ~500 bp upstream. The functional significance of the motif, and whether it relates directly to the repressive element defined by *lin-58* lesions, is as yet unclear. Replacement of the entire 11 bp inverted repeat in *mir-48::gfp* with the AT sequence had the same effect upon GFP expression as did insertion of the *ve33* point mutation; it resulted in enhanced and precocious expression, indicating that the GC repeat is not required for *mir-48* transcriptional activation. In addition, the *lin-58(ve33)* and *lin-58(ve12)* point mutations cause precocious accumulation of miR-48, but do not appear to interfere with the processing of pre-miR-48 (Figures 1B and 1C), suggesting that the site is not required for recruitment of RNA processing machinery. Thus, our data are consistent with a model in which the *lin-58* lesions disrupt a repressor binding site that acts to restrict the timing of microRNA action.

Experimental Procedures

Nematode Strains

Worm strains were grown at 20°C by using standard methods (Sulston and Hodgkin, 1988). *vels51* arose spontaneously, whereas *vels40*, *vels48*, and *vels49* were generated by γ-irradiation. *vels51 let-7(mn112) unc-3(e151)* animals were generated as described in the Supplemental Data. *let-7(mn112)* is a null allele (Reinhart et al., 2000).

Test DNAs and Microscopy

Oligonucleotide sequences used and cloning details are given in the Supplemental Data. pR56 contains the wtA PCR fragment cloned into pCRII (Invitrogen) and confirmed by sequencing. pR58 was derived from pR56 by substituting a fragment containing the *ve33* lesion, and pLM45 contains an additional 0.54 kb upstream of *mir-241*. The QuikChange XL Kit (Stratagene) was used to make the 23 bp miR-48 coding region deletion in pLM48 and the AT replacement in *mir-48(AT)::gfp*. *gfp* constructs were generated in pPD95.67 and injected at 50 ng/μl. Microscopy was performed with a Microphot-FXA (Nikon, Inc., Melville, NY) equipped with differential interference contrast and fluorescence optics. Images were captured with a DVC-1300 camera and were analyzed with DVC C-View 2.1.

Northern Blot Analysis

To synchronize worm cultures, embryos were isolated from gravid adults by hypochlorite treatment. After hatching in M9, worms were plated at low density on NGM plates seeded with *E. coli* OP50, and they were allowed to develop for the indicated times. Total RNA was isolated by using Trizol, and ~20 μg per lane was analyzed by Northern blot as described (Lau et al., 2001). Probes were radiolabeled DNA oligos, and blots were quantified by using phosporimaging (Multi Gauge, Fujifilm), normalizing the counts for each band to the U6 loading control (see Tables S2 and S3). For signals below the detection limit (e.g., the miR-48 in N2, 6 hr), an upper limit was estimated based on the number of counts corresponding to bands just above the detection limit (e.g., the pre-miR48 band in *lin-58*, 32 hr). Thus, the calculation that miR-48 accumulation was 2- to 6-fold higher than wild-type in the 0, 6, and 9 time points was a conservative estimate.

Supplemental Data

Supplemental Data including Northern quantitation, seam cell phenotypes caused by *mir-48* arrays, and additional details on Experimental Procedures are available at http://www.developmentalcell.com/cgi/content/full/9/3/415/DC1/.

Acknowledgments

We thank J. Simon and M. Titus for critical comments on the manuscript and members of the Twin Cities worm community for helpful discussions. We thank A. Abbott, V. Ambros, and their collaborators for insight and communication of results prior to publication. This work was supported by grants from the National Institutes of Health to D.P.B. and A.E.R.

Received: May 6, 2005
Revised: August 3, 2005
Accepted: August 4, 2005
Published: September 6, 2005

References

Abbott, A.L., Alvarez-Saavedra, E., Miska, E.A., Lau, N.C., Bartel, D.P., Horvitz, H.R., and Ambros, V. (2005). The *let-7* microRNA family members *mir-48*, *mir-84* and *mir-241* function together to regulate developmental timing in *Caenorhabditis elegans*. Dev. Cell *9*, this issue, 403–414.

Abrahante, J.E., Miller, E.A., and Rougvie, A.E. (1998). Identification of heterochronic mutants in *Caenorhabditis elegans*: Temporal misexpression of a collagen::green fluorescent protein fusion gene. Genetics *149*, 1335–1351.

Abrahante, J.E., Daul, A.L., Li, M., Volk, M.L., Tennessen, J.M., Miller, E.A., and Rougvie, A.E. (2003). The *Caenorhabditis elegans hunchback*-like gene *lin-57/hbl-1* controls developmental time and is regulated by microRNAs. Dev. Cell *4*, 625–637.

Ambros, V., and Horvitz, H.R. (1984). Heterochronic mutants of the nematode *Caenorhabditis elegans*. Science *226*, 409–416.

Ambros, V., Lee, R.C., Lavanway, A., Williams, P.T., and Jewell, D. (2003). MicroRNAs and other tiny endogenous RNAs in *C. elegans*. Curr. Biol. *13*, 807–818.

Bartel, D.P. (2004). MicroRNAs: genomics, biogenesis, mechanism, and function. Cell *116*, 281–297.

Bartel, D.P., and Chen, C.Z. (2004). Micromanagers of gene expression: the potentially widespread influence of metazoan microRNAs. Nat. Rev. Genet. *5*, 396–400.

Bracht, J., Hunter, S., Eachus, R., Weeks, P., and Pasquinelli, A.E. (2004). Trans-splicing and polyadenylation of *let-7* microRNA primary transcripts. RNA *10*, 1586–1594.

Brennecke, J., Hipfner, D.R., Stark, A., Russell, R.B., and Cohen, S.M. (2003). *bantam* encodes a developmentally regulated microRNA that controls cell proliferation and regulates the proapoptotic gene hid in *Drosophila*. Cell *113*, 25–36.

Brennecke, J., Stark, A., Russell, R.B., and Cohen, S.M. (2005). Principles of microRNA-target recognition. PLoS Biol. *3*, e85.

Doench, J.G., and Sharp, P.A. (2004). Specificity of microRNA target selection in translational repression. Genes Dev. *18*, 504–511.

Feinbaum, R., and Ambros, V. (1999). The timing of *lin-4* RNA accumulation controls the timing of postembryonic developmental events in *Caenorhabditis elegans*. Dev. Biol. *210*, 87–95.

Hobert, O. (2004). Common logic of transcription factor and microRNA action. Trends Biochem. Sci. *29*, 462–468.

Johnson, S.M., Grosshans, H., Shingara, J., Byrom, M., Jarvis, R., Cheng, A., Labourier, E., Reinert, K.L., Brown, D., and Slack, F.J. (2005). RAS is regulated by the *let-7* microRNA family. Cell *120*, 635–647.

Krek, A., Grun, D., Poy, M.N., Wolf, R., Rosenberg, L., Epstein, E.J., Macmenamin, P., da Piedade, I., Gunsalus, K.C., Stoffel, M., and Rajewsky, N. (2005). Combinatorial microRNA target predictions. Nat. Genet. *37*, 495–500.

Lau, N.C., Lim, L.P., Weinstein, E.G., and Bartel, D.P. (2001). An abundant class of tiny RNAs with probable regulatory roles in *Caenorhabditis elegans*. Science *294*, 858–862.

Lee, R.C., Feinbaum, R.L., and Ambros, V. (1993). The *C. elegans* heterochronic gene *lin-4* encodes small RNAs with antisense complementarity to *lin-14*. Cell *75*, 843–854.

Lewis, B.P., Shih, I.H., Jones-Rhoades, M.W., Bartel, D.P., and Burge, C.B. (2003). Prediction of mammalian microRNA targets. Cell *115*, 787–798.

Lewis, B.P., Burge, C.B., and Bartel, D.P. (2005). Conserved seed pairing, often flanked by adenosines, indicates that thousands of human genes are microRNA targets. Cell *120*, 15–20.

Lim, L.P., Lau, N.C., Weinstein, E.G., Abdelhakim, A., Yekta, S., Rhoades, M.W., Burge, C.B., and Bartel, D.P. (2003). The microRNAs of *Caenorhabditis elegans*. Genes Dev. *17*, 991–1008.

Lim, L.P., Lau, N.C., Garrett-Engele, P., Grimson, A., Schelter, J.M., Castle, J., Bartel, D.P., Linsley, P.S., and Johnson, J.M. (2005). Microarray analysis shows that some microRNAs downregulate large numbers of target mRNAs. Nature *433*, 769–773.

Lin, S.Y., Johnson, S.M., Abraham, M., Vella, M.C., Pasquinelli, A., Gamberi, C., Gottlieb, E., and Slack, F.J. (2003). The *C. elegans hunchback* homolog, *hbl-1*, controls temporal patterning and is a probable microRNA target. Dev. Cell *4*, 639–650.

Moss, E.G., Lee, R.C., and Ambros, V. (1997). The cold shock domain protein LIN-28 controls developmental timing in *C. elegans* and is regulated by the *lin-4* RNA. Cell *88*, 637–646.

Ohler, U., Yekta, S., Lim, L.P., Bartel, D.P., and Burge, C.B. (2004). Patterns of flanking sequence conservation and a characteristic upstream motif for microRNA gene identification. RNA *10*, 1309–1322.

Palatnik, J.F., Allen, E., Wu, X., Schommer, C., Schwab, R., Carrington, J.C., and Weigel, D. (2003). Control of leaf morphogenesis by microRNAs. Nature *425*, 257–263.

Pepper, A.S., McCane, J.E., Kemper, K., Yeung, D.A., Lee, R.C., Ambros, V., and Moss, E.G. (2004). The *C. elegans* heterochronic gene *lin-46* affects developmental timing at two larval stages and encodes a relative of the scaffolding protein gephyrin. Development *131*, 2049–2059.

Reinhart, B.J., Slack, F.J., Basson, M., Pasquinelli, A.E., Bettinger, J.C., Rougvie, A.E., Horvitz, H.R., and Ruvkun, G. (2000). The 21-nucleotide *let-7* RNA regulates developmental timing in *Caenorhabditis elegans*. Nature *403*, 901–906.

Rougvie, A.E. (2001). Control of developmental timing in animals. Nat. Rev. Genet. *2*, 690–701.

Seggerson, K., Tang, L., and Moss, E.G. (2002). Two genetic circuits repress the *Caenorhabditis elegans* heterochronic gene *lin-28* after translation initiation. Dev. Biol. *243*, 215–225.

Slack, F.J., Basson, M., Liu, Z., Ambros, V., Horvitz, H.R., and Ruvkun, G. (2000). The *lin-41* RBCC gene acts in the *C. elegans* heterochronic pathway between the *let-7* regulatory RNA and the LIN-29 transcription factor. Mol. Cell *5*, 659–669.

Sulston, J.E., and Hodgkin, J. (1988). The Nematode *Caenorhabditis elegans* (Cold Spring Harbor, NY: Cold Spring Harbor Laboratory Press).

Sulston, J.E., and Horvitz, H.R. (1977). Post-embryonic cell lineages of the nematode, *Caenorhabditis elegans*. Dev. Biol. *56*, 110–156.

Wightman, B., Ha, I., and Ruvkun, G. (1993). Posttranscriptional regulation of the heterochronic gene *lin-14* by *lin-4* mediates temporal pattern formation in *C. elegans*. Cell *75*, 855–862.

Yochem, J., Gu, T., and Han, M. (1998). A new marker for mosaic analysis in *Caenorhabditis elegans* indicates a fusion between hyp6 and hyp7, two major components of the hypodermis. Genetics *149*, 1323–1334.